Remote ECG Monitoring Kit to Predict Patient-Specific Hearth Abnormalities

Jiaming Chen, Abolfazl Razi
School of Informatics, Computing and Cyber Systems, Northern Arizona University
Flagstaff, AZ 86011, USA

ABSTRACT

Electrocardiogram (ECG) signals are widely used to check heart rhythms and general health conditions using low-cost and relatively accurate equipment. However, the majority of commercial off-the-shelf ECG kits are generic and their normal ranges are set based on an average normal hearth signal hence ignorant of extreme variations among different people's normal heart signals. As such, many false alarms are generated if the global thresholds are selected too strict. On the other hand, loosely selected thresholds may result in missing many true alarms. Furthermore, the kits output report typically includes a limited number of basic parameters such as heart rate and hence negligent to a rich set of information exploitable from signal morphology. In this paper, we developed a prototype for patient-specific heart monitoring kit, which learns the properties of a patient's normal ECG signal over time and reports significant deviations from this normal behavior. In order to reduce the false alarm rate even further, the kit is equipped with an accelerometer in order to distinguish between high heart rates due to high physical activity levels and real abnormalities. This personalized remote heat monitoring kit with the proposed signal processing and self-tuning capabilities provides more detailed information and insightful interpretations compared to generic devices, therefore can be used for remote health monitoring of high-risk and elderly people.

Keywords: Personalized Diagnosis, Wearable Sensors, ECG Signal Analysis, Predictive Modeling, Remote Heart Monitoring.

1. INTRODUCTION

Healthcare service in today's society has been significantly improved by using different technological advances such as fully automated diagnosis tools, data-driven predictive modeling and remote monitoring systems. In particular, cardiovascular disease, one of the top ranked killers over the past decades, has been heavily investigated from different perspectives by the biomedical research community [1], [2], [3].

A majority of the mortality rate is due to late diagnosis and delayed theraputic interventions [4]. Therefore, a constant heart condition monitoring and timely predicting of potential heart abnormalities can have a significant impact on saving lives, especially for high-risk patients.

In order to diagnose heart abnormalities, Electrocardiogram (ECG) is widely used in healthcare industry, since it can be implemented using low-cost and affordable circuitry with a relatively high accuracy. Electrocardiograms involve the measurement of electrical activities of different parts of a hearts [3], [5], [6].

Many practical implementations of ECG-based heart monitoring kits in terms of wearable devices (e.g. fitbit [7]), mobile apps (e.g. Alivecor's heart monitor app [8]) as well as more sophisticated commercial cardiac monitoring equipment are developed to assert heart conditions based on ECG signals. However, a majority of these devices suffer from several drawbacks as follows. Firstly, these devices lack advanced signal processing and information extraction capabilities, hence they require result interpretation by an expert. Secondly, the predefined normal ranges for signal parameters (e.g. heart rate) are set based on a typical ECG signal for a normal heart. However, there exists extreme variations among normal heart signals among people, influenced by many factors such as age, gender, race, genetic patterns, as well as environmental conditions (e.g. temperature, elevation from sea level). Therefore, a generic equipment with a pre-defined set of thresholds is not well suited for precise monitoring of different patients' heart functionality. For tightly selected thresholds, the device generates many false alarms. On the other hand, the device may miss significant true alarms for loosely selected thresholds. Thirdly, physical activity of a person has a crucial impact on the ECG signal morphology, which should not be confused with actual hearth abnormalities. This fact is overlooked in the current off-the shelf kits.

In this project, we developed a prototype for a personalized remote heart monitoring kit that probes a patient's heart functionality as well as his physical activity and transmits the collected information to a remote processing unit through wireless communication for further analysis and interpretation.

The design of this system allows a more flexible and continuous cardiac monitoring. The developed learning algorithm builds a patient-specific model to analyze and interpret the ECG signal by detecting deviations from the patient's normal ECG trends. The results of analysis in terms of minor and major alarms are displayed on the kit's display module in order to assist the patient to take proper actions accordingly.

Further, the device is equipped with an accelerometer in addition to ECG measurement probes to incorporate the patient's physical activity into the learning algorithm and avoid false alarm generation due to the patient's physical activities. We also plan to include a web-messaging capability in order to notify the patient's respective health provider in case of severe heart alarms. The results provided in section 4, shows that the developed kit outperforms generic methods based on a global classifier by providing more detailed information about heart functionality and predicting potential upcoming heart abnormalities before their occurrence. This device can be used to remotely monitor heart behavior and general health conditions of high-risk people (such as elderly seniors) and assist patients to take necessary therapeutic actions such as taking rest, calling their doctor and taking their prescribed medications.

The following of this paper is organized as follows. An overview of the entire system is presented in section 2 with elaborating on the details of the designed wearable ECG monitoring module. The proposed signal processing and prediction processing is presented in section 3. The results are presented in section 4, following by concluding remarks in section 5.

2. SYSTEM MODEL

The proposed patient-specific remote heart monitoring kit comprises two modules: a Wearable Sensing Module (WSM) and a computer-based Personalized Processing Unit (PPU). The two

modules communicate using WiFi technology with a simple half-duplex protocol. The WSM module collects analog ECG signal and 3-dimensional accelerometer signal and transmit them to PPU for further analysis. PPU processes the received signals and classifies the received signals into normal and abnormal classes using a global classifier trained using a public ECG dataset. The normal signal segments are used by an online predictive learning algorithm for constant tuning of the patient-specific model parameters. Simultaneously, significant deviations from the normal trend is recognized and presented as minor alarm. The results of processing are sent back to WSM via a feedback channel to be displayed in terms of user-friendly text messages. Fig. 1 shows the block-diagram of the designed prototype. The following sections elaborate on the details of the kit and the developed software.

2.1. Wireless Sensing Module

WSM is designed based on Ardunio Uno microcontroller and includes a single-lead ECG sensing module with three electrodes, an accelerometer and a display module. The ECG electrodes are attached to left arm, right arm, and the lower abdominal cavity. The kit is attached to the arm to maximize sensitivity to physical activities. The analog signals from the two sensors are sampled evenly with sampling rate of 215 samples/sec. WSM receives the feedback messages and displays respective user-friendly text messages on a build-in LCD. Minor and major alarms are shown by two yellow and red LEDs. The displayed messages include the result of signal processing, the patient's physical activity level, the functionality of sensors, and the communication channel status.

2.2. Communication Module

The sensing module constantly collects ECG and three-dimentional accelerometer data and bundles them into transmit packets with the following format. Each packet includes a start flag for flow control, a checksum code for error detection, and the measurement samples. The PPU analyzes the received hyperpacket including 1498 information packets and two control packets and sends back the result of the analysis in a feedback packet, which includes start and end flags, user ID, a set of message codes as shown in Figure 2.

3. SIGNAL PROCESSING AND PREDICTIVE MODELING

The proposed Software is developed in MATLAB Environment with Graphic User Interface (GUI) to facilitate easy data entry (e.g. personal and clinical information), signal processing and result display. In addition to the received signal, a set of representative features as well as the result interpretations are presented. The core part of the software is the proposed learning-based prediction algorithm, which includes the following stages:

1) Data preprocessing and de-noising
2) Segmentation
3) Feature extraction
4) Global classifier
5) Personalized local deviation analysis

De-noising and Baseline removal: Here, we use the popular method of Wavelet decomposition for denoising purpose. We use the 8-level Daubechies wavelet transform (db8), which has been proven to be efficient [9]. Since, we use the public MIT-BIH arrhythmia database with sampling frequency of 360Hz [10] to train the global classifier, we use the relation

$$L = \left\lfloor 1 + \log_2 \frac{Fs}{360} \right\rfloor \quad (1)$$

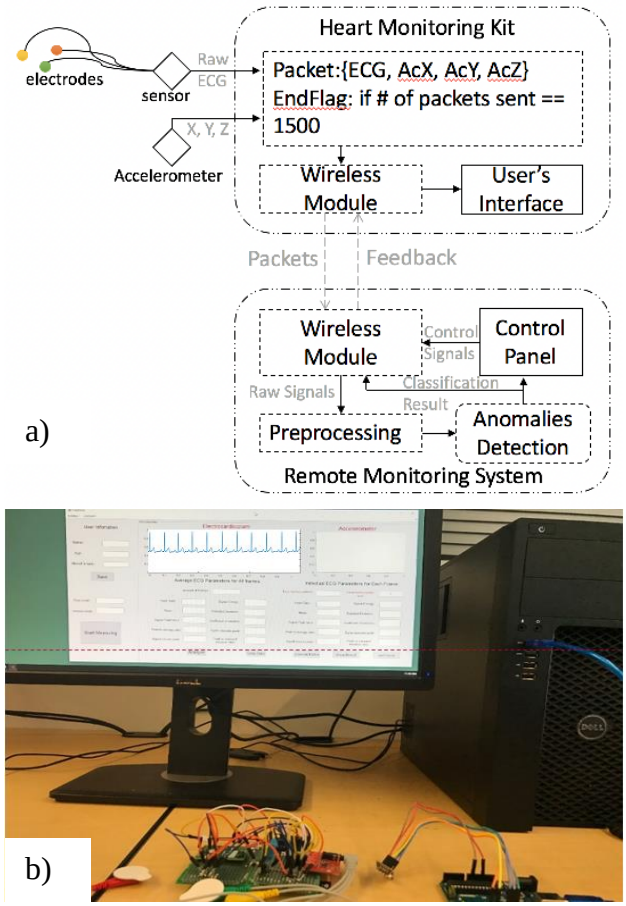

Figure 1: System model. a) conceptual block-diagram, b) the KIT prototype

In order to identify the levels of wavelet transform whose high – frequency details are considered noisy and subject to discard according to the recommendations of the Association for the Advancement of Medical Instrumentation (AAMI) [11]. Here, $\lfloor x \rfloor$ is the floor function and represents the maximum integer number lower than x. To de-noise our ECG signal with sampling rate of $F_s = 215\ samples/sec$, the high frequency details at the first layer is discarded.The baseline wander is another common artifact in ECG signal. In this study, a five ordered fitted polynomial is subtracted from the ECG signal to eliminate the wandering trend. Finally, the resulting signal is resampled to 360Hz to match the training dataset.

Segmentation: We first identify the cardiac cycles using wavelet transform. A typical cardiac circle includes five fiducial peaks, namely P, Q, R, S and T. The QRS complex, which composed of Q, R and S peaks, is the most representative wave of one cycle. The detection of other peaks often depends on the location of QRS complexes. Both normal beats and abnormal beats exhibit QRS complexes in the frequency range of 5 to 22Hz [1]. With a sampling frequency of 360Hz, the detail coefficients of level 4 and level 5 covers the information of QRS complexes. The algorithm described in [10] and [12] using maximal overlap discrete wavelet transform (MODWT) is applied to detect R peaks. We use *db4* as basis function instead of *sym4*, since it exhibits more similarity with a typical QRS complex [1], [9]. The rest of fiducial peaks are then detected within a certain segment around R peaks; resulting in the P, QRS onset, Q, S, QRS offset and T waves within each cardiac circle [1].

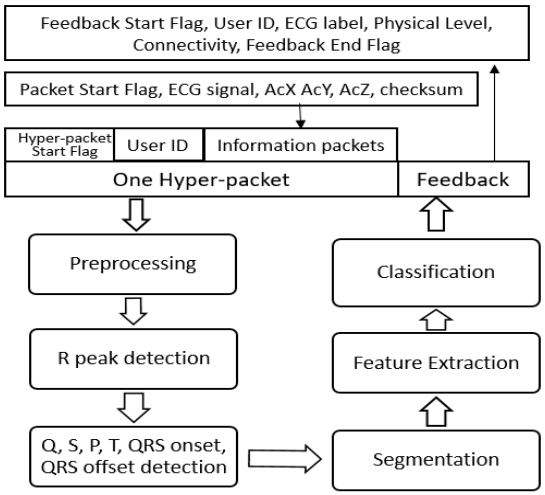

Figure 2: The information and feedback packets.

If p_i is the location of R peak for the i[th] cycle, the range of this cycle is defined as $\left[p_i + \frac{p_i - p_{i-1}}{3}, p_i + \frac{2(p_{i+1} - p_i)}{3}\right]$, noting that R peak approximately splits a cycle of length τ into two parts of length $\tau/3$ and $2\tau/3$ [9]. Further, we combine m consecutive cycles to obtain one analysis segment, in order to eliminate transient artifacts and obtain local averages of signal parameters. In the subsequent learning algorithm, each segment considered as a data-point to be classified. The next segment is obtained by sliding the segment k cycles forward, where $1 \leq k \leq m$. Fig. 3 shows the segmentation concept for $k = 1$ and $m = 3$. It Accelerometer signals are also segmented accordingly.

Feature Extraction: In order to develop an accurate learning algorithm and avoid the well-known overfitting issue, here we extract a set of informative features that capture the main properties of the signals as follows.

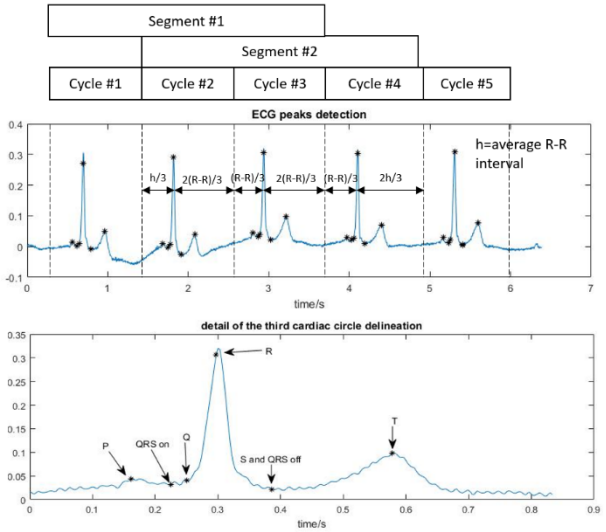

Figure 3: Fiducial peaks of ECG signal. R peaks are used in the segmentation method.

a) For the ECG signal, as depicted in Table. 1, we extract three categories of features including temporal features, morphological features and frequency domain features to make a comprehensive list of features that are reported in the literatures [1] [3] [5] [9]. For each category, we include two sets of features. Set 1 includes 8 features that are calculated per cycle for all m cycles and then we include their mean and coefficient of variations as representative features. Set 2. contains 6 features, which includes general properties of the signal and are calculated once per segment. Therefore, we have a total of $2 \times 8 + 6 = 22$ features. The 22 dimensional feature space is mapped into 8 dimensional space by Principal Component Analysis (PCA). Finally, these 8 features are normalized to yield zero mean unit variance features.

	SET 1	SET 2
Temporal Features	*QRS* duration, *QT* duration, *PR* duration	segment mean *RR*, segment mean$(R_i - R_{avg})$
Morphological Features	max positive peak to second peak ratio	signal average energy, max positive peak, max negative peak, peak to energy ratio
Frequency Domain Features	signal power level at 7.5Hz, 10Hz, 12.5Hz, 15Hz	

Table 1: Features extracted from ECG signal.

For the accelerometer signal, we extract representative features for each segment to build a binary classifier that distinguishes between the active and test modes as presented in Table. 2 following suggestions provided in [13]. For the sake of simplicity, we first combine the three axes of data using the following equation:

$$Ac(i) = \sqrt{AcX(i)^2 + AcY(i)^2 + AcZ(i)^2} \quad (2)$$

If the reading of accelerometer is zero across all axes, then an accelerometer signal loss alarm is displayed.

Metrics Name	Formula
Differences	$\lvert\max\{Ac(i)\}\rvert - \lvert\min\{\mathrm{Ac}(i)\}\rvert$
Stand Deviation	$\frac{1}{N}\sum_{i=1}^{N}(Ac(i) - \frac{1}{N}\sum_{j=1}^{N}Ac(j))^2$
Minimum	$\min\{\mathrm{Ac}(i)\}$
Range	$\max\{Ac(i)\} - \min\{\mathrm{Ac}(j)\}$
Energy	$\frac{\sum_{i=1}^{N}\lvert Ac(i)\rvert^2}{N}$

Table 2: Features extracted from accelerometer signal.

Proposed Personalized Predictive Modeling: In this section, we elaborate on the proposed personalized predictive modeling, which includes two global classifier and local deviation analysis modules under a hierarchical structure as depicted in Fig. 4. In order to verify the proposed algorithm, we apply it to well-annotated MIT-BIH database, which includes two subsets DS1 and DS2, each of which contains ECG signals for 22 patients [11], [14]. Here, we use DS1 as training dataset and DS2 as test dataset. Each ECG signal includes cardiac cycles, which are annotated by experts and mapped into four classes including Normal, Supraventricular, Ventricular and Fusion [5]. The

number of claases in the two database subsets DS1 and DS2 is presented in Table 3.

We first label the ECG segments. A segment is labeled as Normal, if all $m = 3$ member cycles are labeled as *N*, otherwise it is labeled as the only abnormal class *(V, S or F)* within the segment. If a segment includes two or more different abnormal classes, the segment is discarded.

Dataset	# of N segment	# of V segment	# of S segment	# of F segment	Total
DS1	12633	2053	550	121	15357
DS2	11721	2356	862	256	15195
Total	24354	4409	1412	377	30552

Table 3: The Utilized public dataset overview

The following are the details of the global classifier and local deviation analysis module.

a) **Global Classifier:** We first build a global classifier using all segments for all data-points in database DS1. We use k-Nearest Neighbors method with $k = 10$ to build the classifier, since it demonstrates the best performance. However, the method is general and not sensitive to the choice of classifiers.

During the test phase, we process the received signal segments and classify it to one of the four major classes *N*, *V*, *S*, or *F*. The segment at time t is denoted by x_t and the prediction of global classifier is denoted by g_t. The segments that are classified as abnormal ($g_t \in \{V_g, S_g, F_g\}$) trigger a red alarm in the system, while the normal samples $g_t = N_g$ are used to develop an online local model for patient-specific signal properties as presented in Fig. 4.

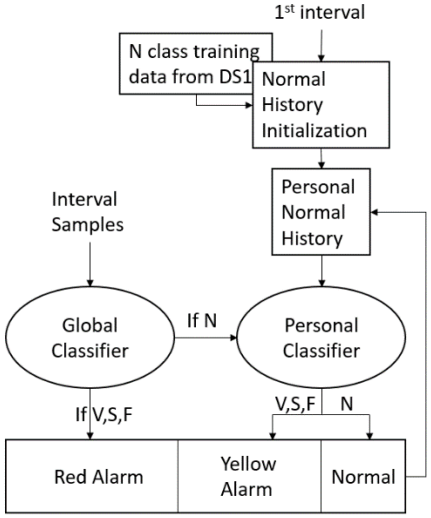

Figure 4: Block-diagram of the proposed predictive model.

b) **The Personalized Deviation Analysis**: This layer is composed of two stages including a deviation detection stage followed by a re-classification stage to obtain final class labels denoted by p_t. The first stage is to verify whether a normally classified sample by a global classifier is a firm normal ($p_t = N$) or leaning towards one of the major alarm classes $\{V, F, S\}$. In the later case, a yellow alarm is triggered based on re-classifying the sample into one of three abnormality classes $p_t \in \{V_p, S_p, F_p\}$.Therefore, the set of the outcome of the whole system is $\{N, V_g, S_g, F_g, V_p, S_p, F_p\}$.

In order to perform the local analysis, we first partition the abnormal samples in the training dataset DS1 (with true labels $\{V, S, F\}$) into three disjoint subsets denoted by $\Omega_V, \Omega_S, \Omega_F$. Then, for a new sample x_t , which is recognized as the following distance metrics:

$$R_{max} = \max_{x_i \in \Omega_N^{(t)}, x_j \in \Omega_N^{(t)}} \left\{ \sqrt[2]{(x_i - x_j)^2} \right\}, \quad (2)$$

$$D_N(x^t) = \underset{x_N \in \Omega_N^{(t)}}{\text{median}} \left\{ \sqrt[2]{(x_t - x_N)^2} \right\}, \quad (3)$$

$$D_V(x_t) = \underset{x_V \in \Omega_V}{\text{median}} \left\{ \sqrt[2]{(x_t - x_V)^2} \right\}, \quad (3)$$

$$D_S(x_t) = \underset{x_S \in \Omega_S}{\text{median}} \left\{ \sqrt[2]{(x_t - x_S)^2} \right\}, \quad (4)$$

$$D_F(x_t) = \underset{x_F \in \Omega_F}{\text{median}} \left\{ \sqrt[2]{(x_t - x_F)^2} \right\}, \quad (5)$$

$$D_{max}(x_t) = \max_{x_N \in \Omega_N^{(t)}} \left\{ \sqrt[2]{(x_t - x_N)^2} \right\}, \quad (6)$$

In the equations above, $D_N(x^t)$, $D_V(x^t)$, $D_S(x^t)$, $D_F(x^t)$ is the median of the distance of the sample x_t from the members of the sets $\Omega_N^{(t)}$, Ω_V , Ω_S and Ω_F , respectively. R_{max} represents the largest pairwise distance for the aggregated normal samples.
The sets of abnormal samples Ω_V , Ω_S and Ω_F are static and developed using the training dataset DS1, whereas $\Omega_N^{(t)}$ is a dynamic set including aggregated normal samples until time t. $\Omega_N^{(t)}$ is an indicator of personal normal history.

In order to improve the accuracy of the local deviation analysis and avoid biasing to the very few first sample, we initialize the set $\Omega_N^{(0)}$ with $n_0 = 300$ normal samples collected from training dataset DS1, which exhibit minimum distance with the first test sample x_0 (n_0 nearest neighbors of x_0 in set DS1). n_0 is chosen

Initialization:
Partition $\Omega^{(DS1)}$ into Ω_N , Ω_S , Ω_V , Ω_P
Set $\Omega_N^{(0)} = \{\ \}$
For $i = 1{:}\, n_0 = 300$
  $\Omega_N^{(0)} = \Omega_N^{(0)} \cup \underset{x \in \Omega_N}{\text{argmax}} (x_0 - x)^2$
End for
For $t = 1 : \infty$
  Calculate $R_{max}, D_N(x^t), D_V(x_t), D_S(x_t), D_F(x_t), D_{max}(x_t)$
  Set $\Omega_N^{(t)} = \Omega_N^{(t-1)}$
  If $(\max(D_N(x_t), D_{max}(x_t)) \le \alpha D_N(x_t))$
    $p_t = N$
    $x_e^{(t)} = \underset{x \in \Omega_N^{(t)}}{\text{argmax}} \sum_{y \in \Omega_N^{(t)}} (x - y)^2$
    $\Omega_N^{(t)} = \Omega_N^{(t)} \setminus x_e^{(t)}$
    $\Omega_N^{(t)} = \Omega_N^{(t)} \cup x_t$
  Else
    $p_t = \theta_y$ with $\theta_y = \underset{\theta \in \{V,S,F\}}{\text{argmin}}\, d_\theta(x_t)$
  End if
End For

based on the average number of normal samples for each patient in dataset DS1.

A sample x_t is deemed normal ($p_t = N$) if we have:

$$\max(D_N(x_t), D_{max}(x_t)) \leq \alpha D_N(x_t), \quad (7)$$

where α is a regularizing parameter. If (7) does not hold, the sample is mapped to a minor abnormality of type $p_t = \theta_y$. We use a k-Nearest Neighbor classifier with $k = 10$ and a square inversion kernel trained using datasets $\Omega_V, \Omega_S, \Omega_F$ [13]. The classification steps can be summarized as:

$$k = 10,\ K(d) = \frac{1}{d^2}, \quad (8)$$

$$d_\theta(x_t) = \sum_{x_j \in \Omega_\theta} K\left(\sqrt[2]{(x_t - x_j)^2}\right), \quad \text{for } \theta \in \{\Omega_V, \Omega_S, \Omega_F\} \quad (9)$$

$$\theta_y = \underset{\theta \in \{V,S,F\}}{\operatorname{argmin}}\, d_\theta(x_t), \quad (10)$$

For subsequent normal samples ($x_t, t \geq 1$), if the new sample x_t is classified as normal ($p_t = N$), then we it joins the set of aggregated normal samples $\Omega_N^{(t)}$ and one member of $\Omega_N^{(t)}$ with maximum average pairwise Mahalanobis distances to the members of this set ($x_e^{(t)} = \underset{x \in \Omega_N^{(t)}}{\operatorname{argmax}} \sum_{y \in \Omega_N^{(t)}} (x - y)^2$) is excluded. is excluded. Therefore, the set $\Omega_N^{(t)}$ accumulates the confirmed normal samples for the patient and is purified over time, hence can be used as a reference to decide the subsequent samples. After running for a couple of minutes, all the samples collected from the training dataset are excluded and the set purely reflects the personal normal history of the current patient. The summary of this algorithm is shown in Fig. 5.

4. RESULTS

In this section, the performance of the proposed method in terms of Classification Accuracy (AC), Specificity (SP) and Sensitivity (SE) is investigated. We first, obtain the classification accuracy by comparing the true labels c_t (expert's annotation) with the outcome of the proposed two-step algorithm p_t. At this step, we combine all abnormalities into one set defined as $\Omega_P = \Omega_V \cup \Omega_S \cup \Omega_F$. Then, we calculate the true positive, true negative, false positive and false negative rates for all test samples. In order to avoid bias to training dataset DS1, we use the 22 unseen samples in DS2 for test purpose. We also, calculate the median and standard deviation values for all performance metrics (AC, SE, SP) in order to examine the robustness of the proposed method and performance variations among 22 test samples. Table 4 summarize the overall results.

Class V	**Median (%)**	**std (%)**
AC	97.57%	18.64%
SE	97.34%	32.05%

Table 4: Classification Accuracy and Sensitivity of the Proposed Method

The results are promising and suggest that with the proposed two-step method with minor alarm recognition capability, the probability of missing a true alarm is negligible. The cost paid is more complexity and reporting minor alarms. There is a tradeoff between the rate of minor alarms and the sensitivity of the method, that can be regularized by tuning regularizing parameter α in equality (7). Here, we used $\alpha = 1$.

In order to analyze the specificity of the method, we consider all classes individually and count the number of calling false alarm types per each class. The results are summarized in Table 5, which demonstrates an excellent specificity per class. In the results presented in Table 4 and Table 5, both minor (yellow) and major (red) alarms are included.

Class V	**Median (%)**	**std (%)**
AC	82.75%	24.99%
SP	99.78%	20.23%
Class S	**Median (%)**	**std (%)**
AC	68.59%	20.24%
SP	99.51%	21.2%
Class F	**Median (%)**	**std (%)**
AC	99.56%	2.47%
SP	100.00%	4.89%

Table 5: Performance measurement 1

From the result presented in Table 4, it's easy to notice that the performance for V and F classes are better, while the performance for class F is more stable compared to class V. This result also is consistent with the fact that class F is a Fusion class and an intermediate state between classes N and V.

A more interesting property of the proposed method is the utility of the minor (yellow) alarms in predicting upcoming major (red) alarms. In order to investigate this property, for each patient, we count the number of subsequent red alarm type that comes after a yellow alarm. The results are shown in Table 6. For instance, the Table suggests that we detect 20 yellow alarms of type S that are followed by a red alarm of type F. Also, the probability of observing major alarms are simply calculated as

$$Probability\ of\ alarm(\theta) = \frac{n_\theta}{n_S + n_V + n_F}, \quad (\theta \in \{S, V, F\}) \quad (11)$$

where n_θ is the number of red alarms of type θ. The results are interesting. For instance, comparing the subsequent major alarms after a yellow alarm V_p reveals that there is 84% chance of having an upcoming red alarm of type V. However, the probability of having an alarm of type V, without considering the yellow alarms is 78%. The same trends holds for all alarm types. This demonstrates an important utility of the yellow alarms, since it means that by detecting yellow alarms, we can predict the upcoming red alarms with a higher certainty. A high-risk patient may take into account these yellow alarms and take cautionary actions (e.g. avoiding physical activity).

	Number of next abnormalities				Probability of next abnormality (%)			
Yellow alarm tag	V_p	S_p	F_p	Total	V_p	S_p	F_p	Total
True V	179	256	4	439	84	75	100	78
True S	30	67	0	97	14	20	0	17
True F	4	20	0	24	2	6	0	4

Table 6: Predictive power of yellow alarms: A yellow alarm increases the chance of observing a red alarm of the same type.

5. CONCLUSIONS

A system is developed for remote heart monitoring. A novel two-step predictive modeling is designed by adding an additional analysis layer to the common approach of using global classifiers. With the proposed method, a normal trend of ECG signal for each patient is learned from the received samples over

time. This trend is subsequently used to trigger minor (yellow) alarms. The results suggest that these yellow alarms are informative in the sense that provides insight about the upcoming major (red) alarms. Since the reaction time in cardiac disease is very important and can significantly reduce catastrophic consequences, the proposed device can be used to notify the users about potential upcoming major alarms in order to take necessary preventive actions.

This kit also can be used to assist the physicians and healthcare staff to interpret the patient's ECG signal more accurately. Finally, by incorporating the accelerometer signal into the predictive modeling, we avoid calling fake alarm due to the patient's physical activities.

References

[1] S. Banerjee, R. Gupta and M. Mitra, "Delineation of ECG characteristic features using multisolution wavelet analysis method," *Measruement,* vol. 45, pp. 474-487, 2012.

[2] L. Lim and B. Yee., "Coach's Companion-Athlete's Health Monitoring System," University of California, Berkeley, 2005.

[3] S. H. Jambukia, V. K. Dabhi and H. B. Prajapati, "Classification of ECG signals using machine learning techniques: A survey.," in *Computer Engineering and Applications (ICACEA), 2015 International Conference on Advances*, IEEE, 2015.

[4] CDC, "State Specific Mortality from Sudden Cardiac Death: United States," *MMWR:1999,* vol. 51, no. 6, pp. 123-126, 2002.

[5] T. Mar and e. al., "Optimization of ECG classification by means of feature selection.," *IEEE transactions on Biomedical Engineering,* vol. 58, no. 8, pp. 2168-2177, 2011.

[6] Y. H. Hu, S. Pelreddy and W. J. Thompkins, "A Patient-Adaptable ECG Beat Classifier Using a Mixture of Experts Approach," vol. 44, no. 9, pp. 891-899, IEEE Transactions on Biomedical Engineering.

[7] "FitBit," [Online]. Available: https://www.fitbit.com/chargehr.

[8] D. Albert, "Two electrode apparatus and methods for twelve lead ECG". USA Patent US 9351654 B2, 31 May 2016.

[9] B. N. Singh and A. K. Tiwari, "Optimal selection of wavelet basis function applied to ECG signal denoising.," *Digital signal processing,* vol. 16, no. 3, pp. 275-287, 2006.

[10] G. B. Moody and R. G. Mark, "The impact of the MIT-BIH arrhythmia database.," *IEEE Engineering in Medicine and Biology Magazine,* vol. 20, no. 3, pp. 45-50, 2001.

[11] ANSI-AAMI, "Testing and reporting performance results of cardiac rhythm and ST segment measurement algorithms.," Association for the Advancement of Medical Instrumentation, Arlington, VA, 1998.

[12] G. B. Moody, "Evaluating ECG analyzers," WFDB Applications Guide, 2003.

[13] D. e. a. Figo, "Preprocessing techniques for context recognition from accelerometer data.," *Personal and Ubiquitous Computing,* vol. 14, no. 7, pp. 645-662, 2010.

[14] P. De Chazal, M. O'Dwyer and R. B. Reilly, "Automatic classification of heartbeats using ECG morphology and heartbeat interval features.," *IEEE Transactions on Biomedical Engineering,* vol. 51, no. 7, pp. 1196-1206, 2004.